# Wavefront sensing for a future HabEx space telescope

Joel Nissen and Stefan Martin
Jet Propulsion Laboratory, California Institute of Technology
Pasadena, California, USA

## ABSTRACT

HabEx is a concept study for a next generation space telescope having a 4 to 6.5 m primary mirror diameter. Primarily designed for exoplanet science, but also carrying general astrophysics instruments, it will have stability requirements orders of magnitude more stringent than any previously flown space-based observatory. Wavefront control, including active sensing/control of wavefront jitter and drift, will be essential to achieving and maintaining coronagraph performance. There are currently two complementary techniques that can be used to sense the wavefront drift. An attractive method is to use starlight rejected from the coronagraph to sense changes in the wavefront incident on the coronagraph mask. This method suffers from photon noise especially when imaging dim stars. It is also unavailable during slews between target stars. Laser metrology is a complementary system in which a laser "truss" enables rigid body displacements of the optics to be measured from changes in the separation of pairs of optical fiducials which can be separated by many meters. In closed loop with actuated optics, laser metrology actively maintains rigid body alignment of the front-end optics, thereby eliminating the dominant source of wavefront drift. This method can maintain rigid body stability of the telescope optics and thereby wavefront control, even during slews between targets.

**Keywords:** HabEx, space telescope, laser metrology

## 1. INTRODUCTION

The HabEx study is defining a concept for a new space telescope with the primary mission of detecting and characterizing planetary systems around nearby stars. The telescope[1] is designed specifically to operate with both a high contrast coronagraph and a starshade, enabling the direct optical detection of exoplanets as close as 70 mas from their star. The telescope will be equipped with cameras for exoplanetary system imaging and with spectrometers capable of characterizing exoplanet atmospheres. Gases such as oxygen, carbon dioxide, water vapor and methane have spectral lines in the visible and near infrared part of the spectrum and may indicate biological activity. In addition to the study of exoplanets, HabEx enables general astrophysics with two dedicated instruments, one a camera/spectrograph (WHC) enabling imaging on a 3 arc minute field of view in two bands stretching from the UV to the near infrared with a multi-object spectrograph mode with resolution of 2000. The second instrument is a high resolution UV spectrograph operating from 120 nm with up to 60,0000 resolution.

HabEx carries two coronagraphs[2][3] (one shown in Fig. 2) covering portions of the science band from 450 to 1000 nm and up to 1800 nm. Stellar coronagraphs work by focusing the light from a star onto a mask, which acts to suppress the starlight at the center of the field while allowing transmission of light form nearby planets. Coronagraphs use "speckle suppression" image-based wavefront sensing and deformable mirrors to tune a "dark hole" around the host star, creating a high-contrast region for planet detection and characterization. Speckle-suppression sensing is an iterative process that relies on long integration times to collect photons from faint residual starlight suppressed by a factor of $10^9$ or more. It is essential that the wavefront is stable for long periods of time or the speckle suppression technique will not converge.

Each coronagraph beam train consists of a fast steering mirror, deformable mirrors for wavefront control, coronagraphic mask, Lyot stop and imaging optics. Also, an integral field spectrograph is included. Within a narrow field, the coronagraph suppresses starlight by a factor of $10^{10}$ or more. To maintain the dark hole, the observatory wavefront error must not drift by more than a few tens of picometers and the line of sight (LOS) jitter must be held below about 0.4 milliarcsec. LOS jitter and wavefront drift must be corrected via feedback to active optics. Starlight rejected at the coronagraph mask or at the downstream Lyot stop is attractive as a control signal source. For example WFIRST coronagraph employs a low order wavefront sensor (LOWFS[4]) in combination with a the coronagraphic mask to sense low order aberrations directly from the starlight, notably tip/tilt and focus. The signals can be fed back to a focus mirror (or a deformable mirror) and a pointing control mirror and subsequently off-loaded to the spacecraft attitude control system. However, this technique has not been demonstrated in the lab for jitter and wavefront control at the $10^{-11}$ contrast level even for bright host stars[5]. The problem will become increasingly difficult as the magnitude of the host star diminishes.

There are two sources for telescope line of sight stability requirements. The first is simple efficiency of light collection so that the point spread function of the starlight remains on the same pixels of the detector to a fraction of the PSF diameter. The second, and a more stringent one, derives from the need to maintain high contrast on the coronagraph which is sensitive to very small wavefront changes. The primary source of wavefront drift will be rigid body displacements of the primary and secondary mirrors relative to coronagraph instrument bench. Simulations have shown that in order to achieve and maintain $10^{10}$ contrast for HabEx, the primary and secondary mirrors must be maintained in six degrees of freedom to nanometer and nanoradian accuracy.

There are two sources of wavefront error to be considered. One arises from the rigid body motion of the telescope and the other from the internal motions of the optics. Naturally, these motions occur at different timescales and the slower motions will be easier to detect. The internal LOWFS sensor does not necessarily directly reveal whether the motion is internal or external. Laser metrology provides a different, complementary sensing method, one that can be used to measure changes in the alignment of the optics independent of the magnitude of the host star. It measures the relative positions of the three mirrors of the telescope. In closed loop with actuators, MET thus provides active alignment of the front-end optics, thereby eliminating the dominant internal source of wavefront drift and LOS jitter. Because laser metrology has ample photons, unlike detectors that rely on rejected starlight, it can operate at high bandwidth and feed forward LOS errors to a fast-steering mirror correcting internally generated spacecraft disturbances.

## 2. TELESCOPE DESIGN

The telescope is a three mirror anastigmat (TMA) with a 4 m diameter primary mirror, 2.5 m off axis, producing a collimated 50 mm diameter beam at the output. The collimated output greatly simplifies the accommodation of the instruments, since otherwise, off axis optics would be needed throughout the systems. Figure 1 shows the telescope layout. Instruments are arranged near the tertiary mirror. By placing smaller fold mirrors between the tertiary and the exit pupil, individual fields of view can be extracted and passed to the instruments. This design allows different optical coatings on the tertiary to aid transmission efficiency with some instruments. Since the telescope has to work into the UV, a protected aluminum coating is required on at least the first two mirrors.

Figure 2 shows part of the coronagraph instrument After striking the tertiary mirror, the rays are collimated and converge towards an on-axis pupil plane. Before reaching that plane however, the beam is extracted by a fold mirror and directed to a fine steering mirrors (FSM) located at a pupil plane. The FSM is used for fine pointing correction based on the output of a wavefront sensor within the coronagraph.

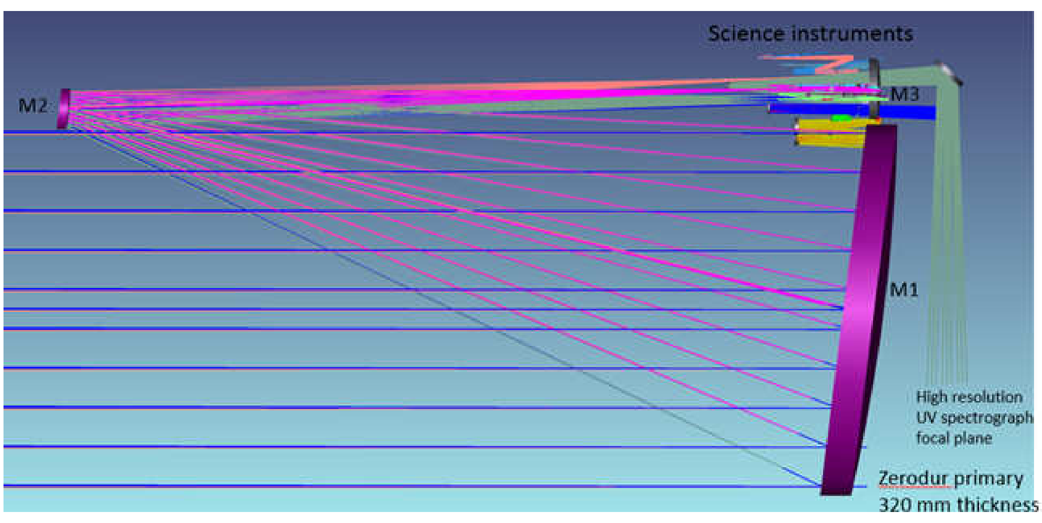


Figure 1: HabEx space telescope optical system. Science instruments are arranged near the primary mirror to reduce the moment of inertia and improve stability.

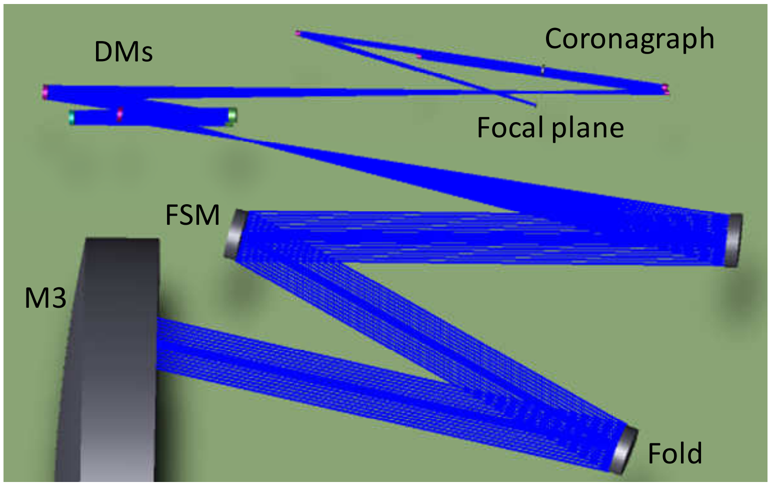


Figure 2: Part of the coronagraph layout showing beam coming from tertiary mirror M3, FSM used for fine pointing control and DMs used for wavefront correction.

**Telescope LOS stability**

The effect of disturbances to the positions of the optics was calculated by displacing and rotating each of the first three mirrors in 6 degrees of freedom and the output beam direction calculated. Table 1 shows one possible allocation of rigid body motions to reach pointing accuracy of ~2 mas rms. The allocation is based on both on performance and on the measurement capability of the laser gauges described below. This allocation does not include an allocation for thermal or dynamic effects on the structure. A more detailed analysis, albeit one that excludes metrology considerations, is presented in [6].

Table 1: Displacement allocations for the three mirrors of the TMA that together produce a 2.2 mas rms on sky pointing error, and produce measurable metrology signals . DX or DY signifies a move across the optical axis. TX or TY signifies a tilt around the X or Y axis passing through the nominal chief ray intercept (CRI) on the mirror surface. DZ is a move along the optical axis and TZ a rotation of the optic around the CRI. The telescope has symmetry across the Y-Z plane. The secondary mirror CRI is displaced in the +Y direction from the primary mirror CRI. “nr” signifies nano-radian

| **Optic** | **M1** | | | | **M2** | | | | **M3** | | | |
|---|---|---|---|---|---|---|---|---|---|---|---|---|
| **Move** | DX,DY | DZ | TX,TY | TZ | DX,DY | DZ | TX,TY | TZ | DX,DY | DZ | TX,TY | TZ |
| **Unit** | nm | nm | nr | nr | nm | nm | nr | nr | nm | nm | nr | nr |
| **Allocation** | 10 | 60 | 10 | 10 | 10 | 60 | 60 | 100 | 10 | 120 | 50 | 200 |

To reach such stability will require active control of the optics. In a passive scenario, a low CTE telescope truss structure would be monitored by temperature sensors and maintained to the 1 mK level to preserve alignment. However, such a scheme would not be proof against effects such as outgassing of a composite telescope structure. A laser metrology truss tying the first three optics together can sense internal drift of the optics, then actuators can be used to restore alignment. Such a system has other benefits too, such as the ability to hold the telescope setup precisely when moving between a bright star used to set up the coronagraph deformable mirrors and the target, or between target stars.

**Laser gauges**

Laser metrology for large coronagraph-equipped space-born observatories was first proposed for the Terrestrial Planet Finder Coronagraph[7]. The beam launcher transmits a collimated beam through free space to a corner-cube retroreflector. The reflected beam couples back into the beam launcher where it mixes with a reference beam and is coupled into a fiber optic. The current generation of laser metrology (MET) has single-digit nm measurement error at 1 kHz sampling and single-digit nm/°C temperature coefficient.

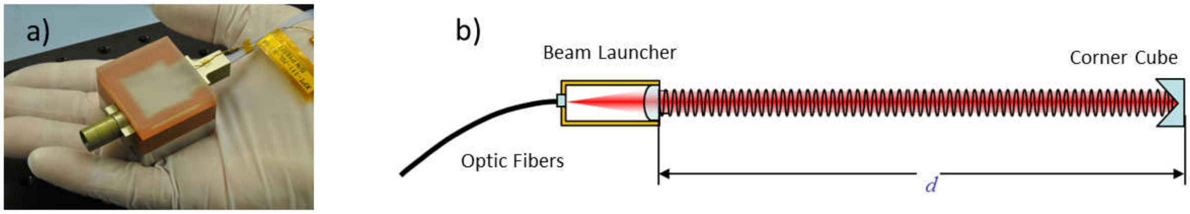


Figure 1. a) The beam launcher and optics bench are built into a small planar lightwave circuit (PLC) suitable for mounting on lightweight-active telescope optics. b) Principle of a laser gauge. Phase modulated laser light is delivered to a beam launcher via fiber optics. The beam launcher collimates the laser light and directs it in free space to a corner cube retroreflector. The returned beam is coupled back into fiber optics and the heterodyne signal is detected with photodiodes. The metrology gauge measures displacement between the vertex of the corner cube and a fiducial surface inside the beam launcher.

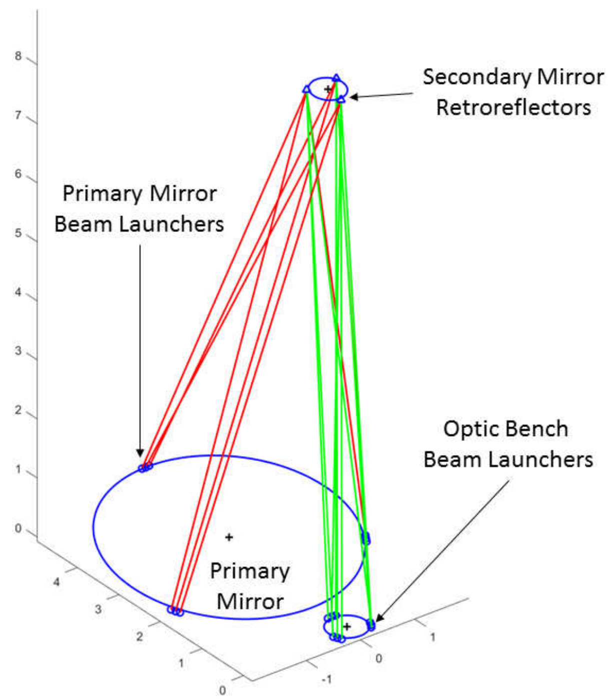


**Figure 3: HabEx laser metrology truss. Beam launchers are placed at the primary and tertiary mirrors and reflect from common retroreflectors located at the secondary mirror. The primary and secondary mirrors are mounted on rigid body actuators which are actively controlled in closed loop with laser metrology. Laser metrology truss**

An optical truss can be constructed to detect rigid body motion of one optic relative to another. Six gauges arranged in a hexapod are sufficient to detect displacements in all six degrees of freedom. By actuating the optic, alignment can be maintained with a feedback loop closed around the laser metrology. Figure 3 illustrates the combination of two optical trusses to stabilize a primary and secondary mirror relative to the tertiary mirror. In this model, hexapods are replaced with nonapods to provide redundancy. In total, eighteen metrology gauges control twelve degrees of freedom. Because each laser gauge requires only a microwatt of power, all the gauges can be supplied by a single 1.55-micron laser source.

The geometry of the truss determines the sensitivity of the measurements to each degree of freedom. Long, narrow trusses are sensitive to tip, tilt and piston but insensitive to lateral translation and in-plane rotation of the optic.

With expected rms gauge error of 0.15 nm or better, the rms wavefront error will be less than 5 pm, keeping the contrast drift below $1\times10^{-11}$ at 500 nm (based on contrast simulations analyzed using PROPER[8])  The exact contrast is a function of coronagraph type: a charge 4 vector vortex coronagraph (VVC) is much less sensitive to tip/tilt than a hybrid Lyot with band-limited mask. However, because of the finite stellar diameter (~1 mas for a G type star at 10 pc) even with the charge 4 VVC, pointing jitter as low as 0.4 mas is required[5]. In summary, both sensing and correcting rigid body motion of the front end optics will be required to maintain a high contrast dark hole. A laser metrology truss also provides stabilization when moving between stars.

**RMS wavefront error requirements and budget**

One possible metrology gauge error budget is shown in Fig. 4. In this example, the main contributor from the beam launcher is the thermal drift showing that good thermal control is required and the beam launcher itself dominates the budget. The current generation of beam launchers is expected to meet the HabEx contrast drift goal with ~20 mK thermal control (Fig. 5).

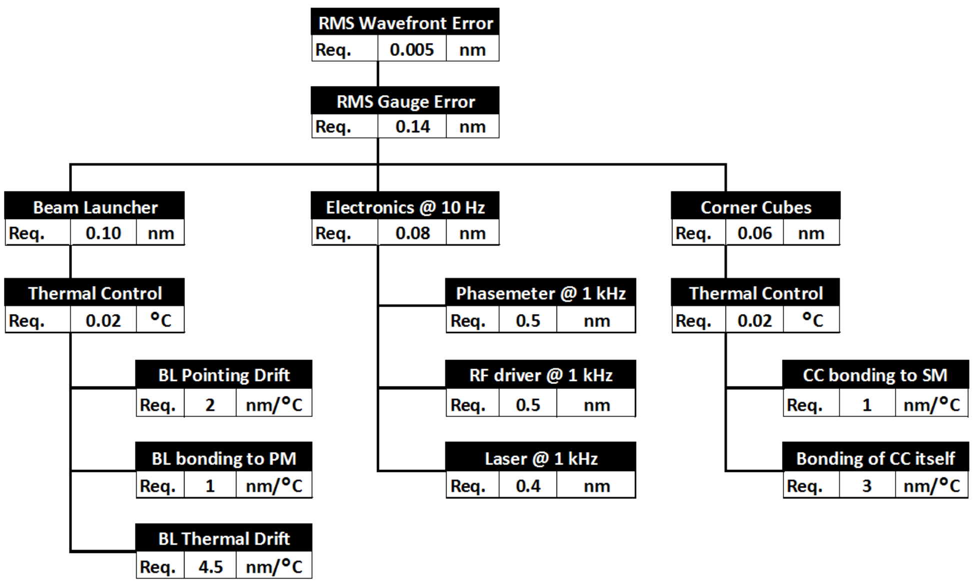


Figure 4: MET error budget for the HabEx 4 meter aperture monolithic observatory. The beam launcher, corner cube, and interface sensitivities have been demonstrated in a flight-like environment. The thermal control loop requirement is achievable due to the compact size of the MET hardware and the benign environment dictated by the necessity of thermal control for the optics in contact with the MET hardware. The phase noise is based on a simple zero-crossing phase detector.

Given gauge performance consistent with the budget, Table 1 shows the RMS wavefront error in terms of low order aberrations. These aberrations interact differently with different coronagraph types.

**Pointing control**

HabEx will use the WHC to provide telescope pointing referenced to guide stars. This will allow pointing to ~ 2 mas. The finer pointing control required by the coronagraphs will be done with the FSM based on the signal from the internal Zernike wavefront sensor.  Fractional milliarcsec jitter is needed to prevent contrast degradation caused by stellar leakage around the mask. This low jitter can be achieved for HabEx by using electric microthrusters rather than reaction wheels. An alternative would be active or passive telescope isolation from the spacecraft bus. Further improvement can be gained by sampling the MET at 5 kHz to estimate the LOS jitter of the front end optics and then feeding the error to the FSM in a feed-forward loop. The simple zero-crossing phasemeter, which was adequate to correct thermally induced rigid-body disturbances, is not adequate to sense LOS jitter within the required bandwidth.  LOS jitter control at the nanoradian level will demand a low noise phasemeter such as developed for Grace Follow-on[9].

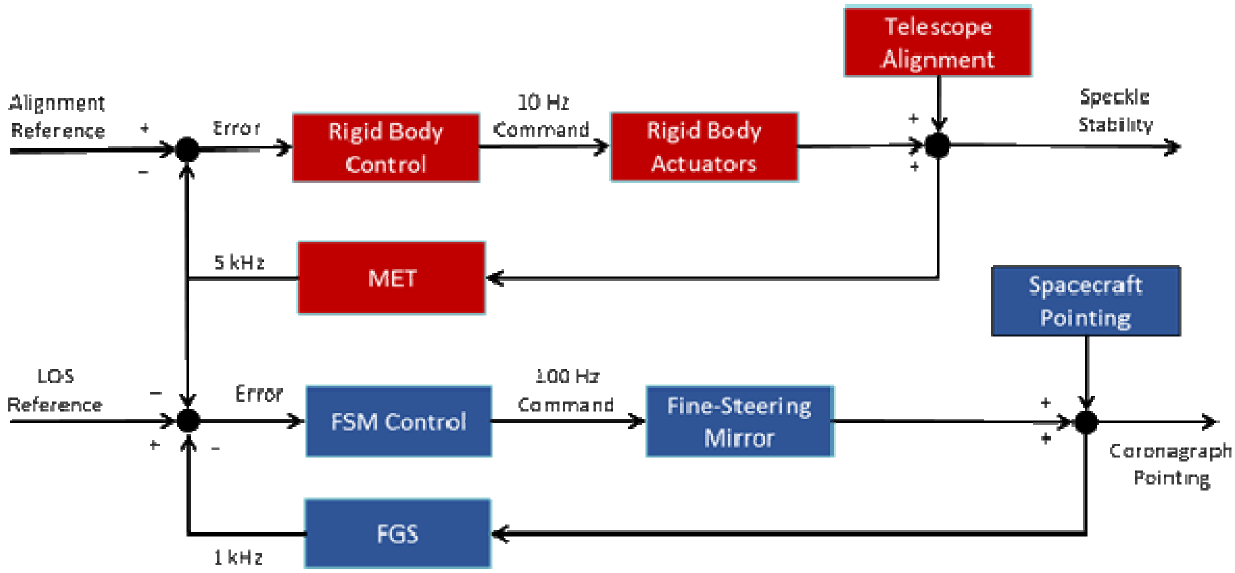


Figure 5: Because laser metrology is only sensing the alignment of the primary and secondary mirrors relative to the optic bench, MET must be supplemented by a line-of-sight control loop. Telescope pointing is controlled by the WHC and the microthrusters to the 2 mas level and a Fine Guidance Sensor (FGS) measures starlight rejected by the coronagraph to detect misalignment between the stellar image and the coronagraph mask to sense at the sub milliarcsec level. The line-of-sight error is corrected with a Fine-Steering Mirror (FSM) located upstream of the deformable mirrors. The LOS control loop corrects for spacecraft (SC) pointing errors as well as residual errors from the MET control loop and LOS errors from optics downstream of the tertiary mirror.

**Contrast and wavefront aberrations**

Random errors were applied to the metrology gauges consistent with 0.02°C thermal control of the beam launchers, retroreflectors and interfaces. The resulting wavefront errors were fit to the first 40 Zernike coefficients according to Noll ordering. As can be seen in Figure 6, the residual wavefront error, due to rigid body motion of the primary and secondary mirror, do not generate large amplitude, high-order Zernike terms. For a monolithic primary, the piston term, Z1, can be neglected and the LOS terms, Z2 and Z3 can be greatly reduced by the FGS control loop. The focus term is two orders of magnitude smaller than the MET gauge error, indicating that the high-contrast field can be maintained with 150 pm of gauge error.

Sensitivity to different misalignments of the optics varies with coronagraph type. The focus term, which dominates the post-MET residual errors (Figure 6) is strongly suppressed in vector vortex coronagraphs (VVC). VVC coronagraphs are less sensitive to  jitter than HLC, particularly the VVC charge 6, but this degrades the throughput for small inner working angles, so planet-finding performance for inner rocky planets would suffer.

To assess the effectiveness of laser metrology for the HabEx baseline 4 meter unobstructed aperture, a 10% bandwidth charge-6 vector-vortex coronagraph was modeled and tuned to produce $10^{-10}$ contrast between an IWA of 2.5 λ/D and an outer working angle of 11 λ/D, where λ is the central wavelength (550 nm). Surface roughness of the front-end optics was simulated with a 2D power spectral density with 8 nm RMS WFE. Figure 7 illustrates an observing sequence that tales advantage of the extraordinary stability of the HabEx.  An exposure is acquired in which a single planet is hidden in the residual speckle of the high contrast region. After a 30° roll of the spacecraft, a second exposure is acquired. Because the speckle pattern rolls with the telescope it is stationary on the focal plane, and differencing the two images suppresses the speckle revealing the planet.


Figure 6: A charge 6 vector-vortex coronagraph is insensitive to low-order Zernike terms Z1-Z8 and Z11, but is not effective in suppressing the higher order terms. The worst offenders, Z2 and Z3, line-of-sight errors, are corrected by the fine guidance control loop. For the unobscured HabEx design, high order Zernike terms, due to rigid body motion of the primary and secondary mirrors, are not produced with amplitudes large enough to affect the contrast.

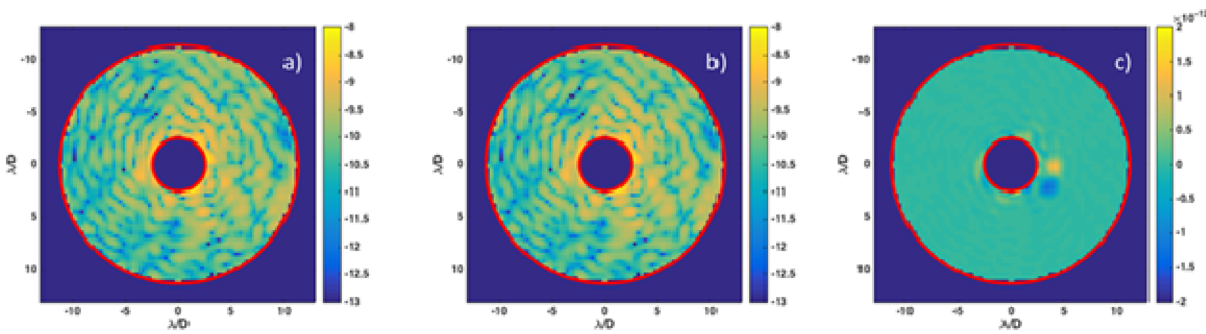


Figure 7. Simulation of an exposure of the 4-meter HabEx high-contrast region containing a single exoplanet. The alignment state is maintained by a MET control loop based on the error budget of figure 3. The dark hole was tuned for $2 \times 10^{-10}$ raw contrast between IWA = 2.5 λ/D and OWA = 11 λ/D (red circles). 4a) The first exposure (illustrated here as contrast on a logarithmic scale) in which the planet is buried in the speckle. 4b) After a 30° roll maneuver, a second exposure is taken. The speckle rotates with the focal plane so it appears stationary. 4c) The difference between the two images plotted on a linear scale. The exoplanet appears as a positive detection and a negative detection rotated by 30°.

## 3. CONCLUSION

High contrast coronagraphy on the next generation of large, coronagraph-equipped, space-borne observatories will require an unprecedented level of stability, not achievable through passive or thermal control systems. The proposed HabEx architecture uses an unobscured aperture and coronagraphs designed to be insensitive to low-order wavefront errors and microthrusters to mitigate wavefront drift and LOS jitter. In addition, wavefront sensing of starlight rejected by the coronagraph will be necessary to achieve the required stability. This is a powerful technique, but has sensing limitations in that individual optic contributions are not resolved, and performance will be photon limited for many stars.

Internal laser metrology is a complementary technique to wavefront sensing, indeed by internally sensing and controlling the telescope optics wavefront sensing performance and speed requirements can be significantly relaxed. This hierarchical approach has the bandwidth, stability and resolution needed to maintain high-contrast zones during the long exposures needed for detection and characterization of exoplanets.


**Acknowledgement**

This work was conducted at the Jet Propulsion Laboratory, California Institute of Technology, under contract with the National Aeronautics and Space Administration.


Copyright 2017 California Institute of Technology. Government sponsorship acknowledged. All rights reserved.


***References:***


[1] Stefan Martin, Mayer Rud, Paul Scowen, Daniel Stern, Joel Nissen, John Krist, "HabEx space telescope optical system" Proc. SPIE 10398, September 2017.

[2] John Trauger; Dwight Moody; John Krist; Brian Gordon, 2015, "Hybrid Lyot coronagraph for WFIRSTAFTA: coronagraph design and performance metrics", J. Astron. Telesc. Instrum. Syst. 2016.

[3] Dimitri Mawet, Laurent Pueyo, Dwight Moody, John Krist, Eugene Serabyn, "The Vector Vortex Coronagraph: sensitivity to central obscuration, low-order aberrations, chromaticism, and polarization". Proc. SPIE 7739.

[4] Fang Shi, Kunjithapatham Balasubramanian, Randall Bartos, Randall Hein, Brian Kern, John Krist, Raymond Lam, Douglas Moore, James Moore, Keith Patterson, Ilya Poberezhskiy, Joel Shields, Erkin Sidick, Hong Tang, Tuan Truong, Kent Wallace, Xu Wang, Dan Wilson, "Low order wavefront sensing and control for WFIRST-AFTA coronagraph". Proc. SPIE 9605, November 2015

[5] Fang Shi, Eric Cady, Byoung-Joon Seo, Xin An, Kunjithapatham Balasubramanian, Brian Kern, Raymond Lam, David Marx, Dwight Moody, Camilo Mejia Prada, Keith Patterson, Ilya Poberezhskiy, Joel Shields, Erkin Sidick, Hong Tang, John Trauger, Tuan Truong, Victor White, Daniel Wilson, Hanying Zhou, "Dynamic testbed demonstration of WFIRST coronagraph low order wavefront sensing and control (LOWFS/C)," Proc. SPIE 10400, 2017.

[6] H. Philip Stahl,, "Overview of a telescope concept design for the Habitable-zone Exoplanet Direct Imaging Mission", Proc. SPIE 10398, September 2017.

[7] Shaklan, S. B., Marchen, L. F., Zhao, F., Peters, R. D., Ho, T. and Holmes, B., "Metrology system for the Terrestrial Planet Finder Coronagraph," Proc. SPIE 5528, Space Systems Engineering and Optical Alignment Mechanisms, 22 (September 30, 2004); doi:10.1117/12.559998.

[8] John E. Krist, "PROPER: an optical propagation library for IDL", Proc. SPIE 6675, September 2007.

[9] Bachman, B. et al, "Flight phasemeter on the Laser Ranging Interferometer on the GRACE Follow-On mission" IOP Conf. Series: Journal of Physics: Conf. Series 840 (2017) 012011